

# Modeling CUBES: from instrument simulation to data reduction prototype

A. Scaudo<sup>a,b</sup>, M. Genoni<sup>a</sup>, G. Cupani<sup>c</sup>, M. Porru<sup>c</sup>, G. Calderone<sup>c</sup>, R. Smiljanic<sup>d</sup>, M. Landoni<sup>a</sup>,  
R. Cirami<sup>c</sup>, and S. Covino<sup>a</sup>

<sup>a</sup>INAF– Osservatorio Astronomico di Brera-Merate, via E. Bianchi 46, I-23807 Merate (LC),  
Italy;

<sup>b</sup>University of Insubria, Via J.H. Dunant, 3, 21100 Varese, Italy;

<sup>c</sup>INAF - Osservatorio Astronomico di Trieste, via G. B. Tiepolo 11, 34131 Trieste, Italy;

<sup>d</sup>Nicolaus Copernicus Astronomical Ctr., ul. Bartycka 18, 00-716 Warszawa, Poland;

## ABSTRACT

We present a comprehensive overview of the collaborative efforts between the End-to-End (E2E) Simulator and the Data Reduction Software (DRS) team, focusing on the modeling of the U-band efficient Cassegrain spectrograph CUBES (ESO-VLT). The E2E model is a Python-based numerical simulator capable of rendering synthetic raw frames with high precision for both astronomical and calibration sources, starting from their 1-d radiation spectra up to the data produced by the detectors. Data from the E2E are processed by the prototype Data Reduction Software (pDRS), a Python library which implements the critical algorithms of the DRS. The PDRS performs wavelength calibration and extracts a 1-d spectrum from one or more reduced science exposures. The 1-d spectrum produced by the extraction routine is meant to be compared directly with the input spectrum fed to the E2E, actually “closing the loop” allowing for a real end-to-end assessment of the instrument capabilities.

**Keywords:** ESO-VLT telescope – CUBES - End-to-End simulations – Data Reduction Software

## 1. INTRODUCTION

The Cassegrain U-Band Efficient Spectrograph (CUBES) is a cutting-edge instrument being developed to be installed in one of the Unit Telescopes (UT1, UT2, or UT3) of the Very Large Telescope (VLT) at the European Southern Observatory (ESO). CUBES aims to maximize efficiency at a spectral resolving power ( $R$ ) greater than 20,000, targeting the bluest part of the spectrum accessible from the ground (300 nm to 400 nm) while being designed to achieve a high instrumental efficiency, exceeding 37%. Given its performance at short wavelengths, CUBES will provide an unprecedented blue eye on the sky alongside the Extremely Large Telescope (ELT) that is now under construction on Cerro Armazones.<sup>1</sup> CUBES promises a tenfold increase in sensitivity compared to current near-UV instruments, enabling groundbreaking across a broad range of scientific topics. These include the search for water in the asteroid belt,<sup>2</sup> studies of stellar evolution and nucleosynthesis, and investigations into the contributions of galaxies and active galactic nuclei to the cosmic UV background. The successful development of CUBES involves a phased approach, allowing for trade-offs between requirements and hardware configurations to optimize performance and meet scientific goals. During the final design phase (Phase C), the End-to-End (E2E) simulator tools<sup>3</sup> — including both science and technical versions — played a critical role.

E2E simulators are sophisticated software systems that mimic the instrument’s behavior during astronomical observations, from the flux distribution of scientific sources to the raw data output by the detector. Synthetic raw frames generated by the E2E simulations contribute to the development of the Data Reduction Software (DRS), facilitating an initial evaluation of the project’s scientific goals and providing feedback to the technical team during design phases and trade-off studies.

During Phase C, data produced by the technical version of the E2E simulator were processed by the prototype Data Reduction Software (pDRS), a Python library implementing essential DRS algorithms. The pDRS handles tasks such as wavelength calibration and extraction of a 1D spectrum from reduced science exposures. This 1D spectrum is then compared with the input spectrum provided to the E2E simulator, effectively “closing the loop”

and enabling a comprehensive assessment of the instrument's capabilities. This iterative process also allowed for improvements in the E2E simulations products and the development of the pDRS pipeline.

The CUBES instrument is also equipped with an Active Flexure Compensation (AFC) system to compensate for thermo-gravitational flexures occurring on the CCD, maintaining an average accuracy within 0.5 pixel. The system uses a Thorium-Argon (ThAr) lamp and fiber to illuminate the AFC aperture, positioned outside the area designated for science and simultaneous calibration spectra. Cross-correlation is performed between a reference daytime high signal-to-noise AFC spectrum and the night-time AFC spectrum to identify any shifts. If these shifts exceed a certain threshold, a correction is applied. The E2E simulator has been crucial in evaluating the precision and accuracy of the cross-correlation algorithm by providing the necessary AFC frames to detect shifts in both spatial and spectral directions.

This paper is organized as follows: Section 2 describes the CUBES instrument, detailing its current design. Section 3 discusses the technical version of the End-to-End (E2E) simulator, highlighting its architecture and functionalities. Section 4 focuses on the Active Flexure Compensation (AFC) system and the results obtained from testing the cross-correlation algorithm. Section 5 covers the data reduction software iteration, describing the tested recipes. Finally, Section 6 concludes with a summary of the results and future directions.

## 2. THE CUBES INSTRUMENT

CUBES will be mounted in one of the Unit Telescope (UT1, UT2 or UT3) at the VLT's Cassegrain focus, and its instrument baseline is composed of several components. These include a front-end unit, which incorporates an acquisition and guiding path. A fore-optics subsystem that encompasses an atmospheric dispersion corrector (ADC), and a re-imaging unit that projects the light to the image slicer. The instrument, in fact, features two image slicers to enable different resolutions. and a calibration unit. Finally, CUBES has two spectrograph arms: arm 1 (blue-optimized) and arm 2 (red-optimized). Both arms are equipped with transmission gratings that have a high groove density, working at the first order, and  $9k \times 9k$  scientific detectors.

Being a Cassegrain Instrument, CUBES will be affected by gravitational flexure according to the telescope orientation during science observations. In addition, also thermal effects are relevant since CUBES is not a temperature stabilized instrument like the ones operating in a (vacuum) vessel. Therefore, its design foresees the implementation of active flexure compensation, in order to cope with differential flexures between the slicer output focal plane and the detector plane.

A detailed description of the CUBES instrument is outside the scope of this paper; refer to<sup>4</sup> for more information. Here, we briefly outline its main characteristics and subsystems, as illustrated in the functional schematic of Fig 1.

### 2.1 Front-end

The front-end includes the Acquisition and Guiding (A&G) subsystem, which handles the initial acquisition of the science target and provides secondary guiding capabilities during exposure.

### 2.2 Fore-optics

The fore-optics subsystem produces a collimated beam for the ADC and magnifying optics, which then supply the image slicer. The image slicer reformats the science object into narrower slits at the spectrograph's input, allowing for higher resolution than a traditional slit. Two image slicers are included, offering both high- and low-resolution modes (HR and LR, respectively).

### 2.3 Calibration Unit

The Calibration Unit provides light sources for various calibration procedures, including flat fielding, wavelength calibration, simultaneous wavelength calibration, alignment, and sources for the Active Flexure Compensation functionality.

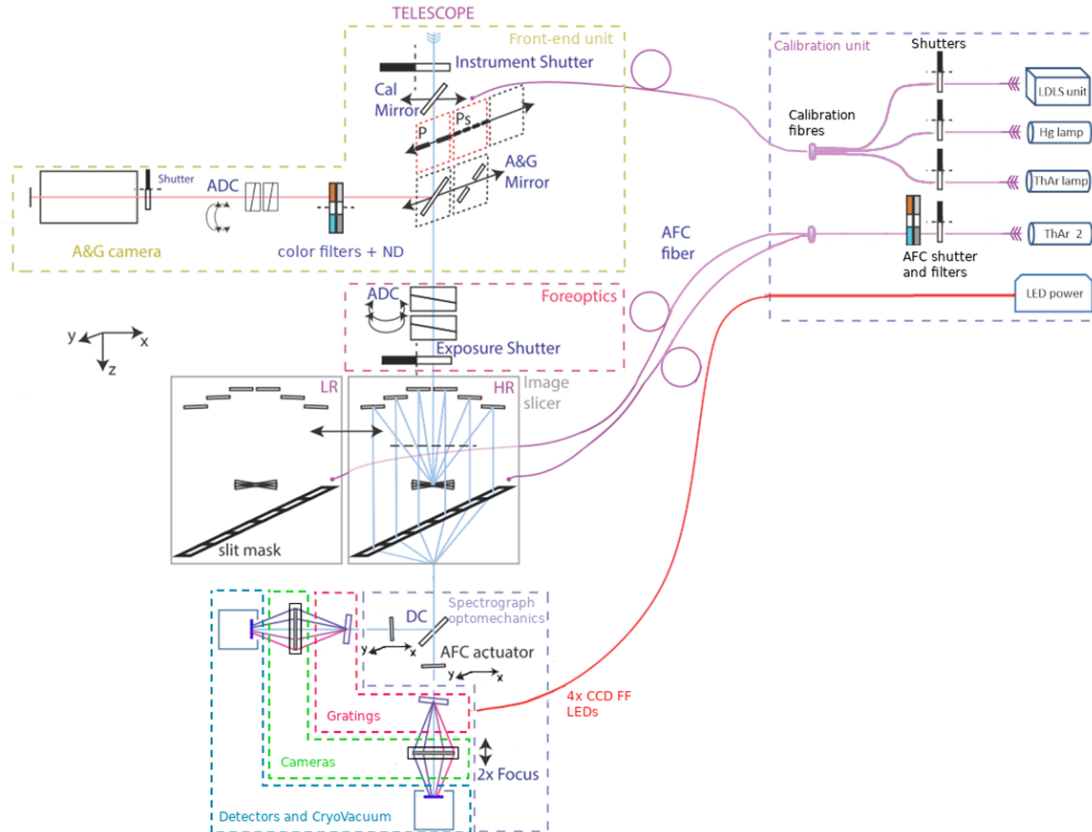


Figure 1: CUBES architecture and functional diagram. Functions are represented via icons and geometries, Subsystem/product decomposition is indicated by dashed regions.

## 2.4 The spectrograph

The spectrograph subsystem consists of two arms. Each arm collimates the beam, disperses the light using a transmission grating, and refocuses the image with a camera onto a 9k x 9k scientific detector. The design also includes actuators for the AFC System.

## 3. END-TO-END SIMULATOR

The End-to-End Instrument simulator (E2E) is a tool which aims to simulate the instrument behaviour and the astronomical observations from the radiation of the scientific sources (or calibration sources in the case of calibration frames) to the raw-frame data produced in output by the instrument detectors. Its purposes are:

- Production of sets of synthetic full raw-frame to aid the development of the DRS, for which the capability of producing synthetic calibration raw-frames is fundamental
- Ad-hoc simulations to give useful feedback during design phases
- Generation of synthetic full raw-frame to allow first science evaluation of scientific goals

Two different versions, targeted for different uses and users are under development:

- Science Version: for first science evaluations and preliminary performances

- Technical Version: for higher accuracy simulations to be exploited for DRS development and to aid in evaluating instrument design and performances.

In the following subsections, the technical version, referred to as the End-to-End simulator (E2E), is presented. The E2E aims to produce high-accuracy simulations, including detailed spectral traces of different slices, optical PSF blurring contributions, and detector diffusion effects. These simulations are primarily intended for DRS development, with the continuous enhancement of the E2E version driven by ongoing collaboration with the DRS Work Package. The architecture is highly modular, consisting of various modules, units, and interfaces, as outlined in the schematic workflow of Fig. 2. The simulator is developed in Python 3.9, utilizing specific libraries for specialized functionalities and interfacing with other software, such as the commercial optical ray tracing tool Zemax-OpticStudio®.

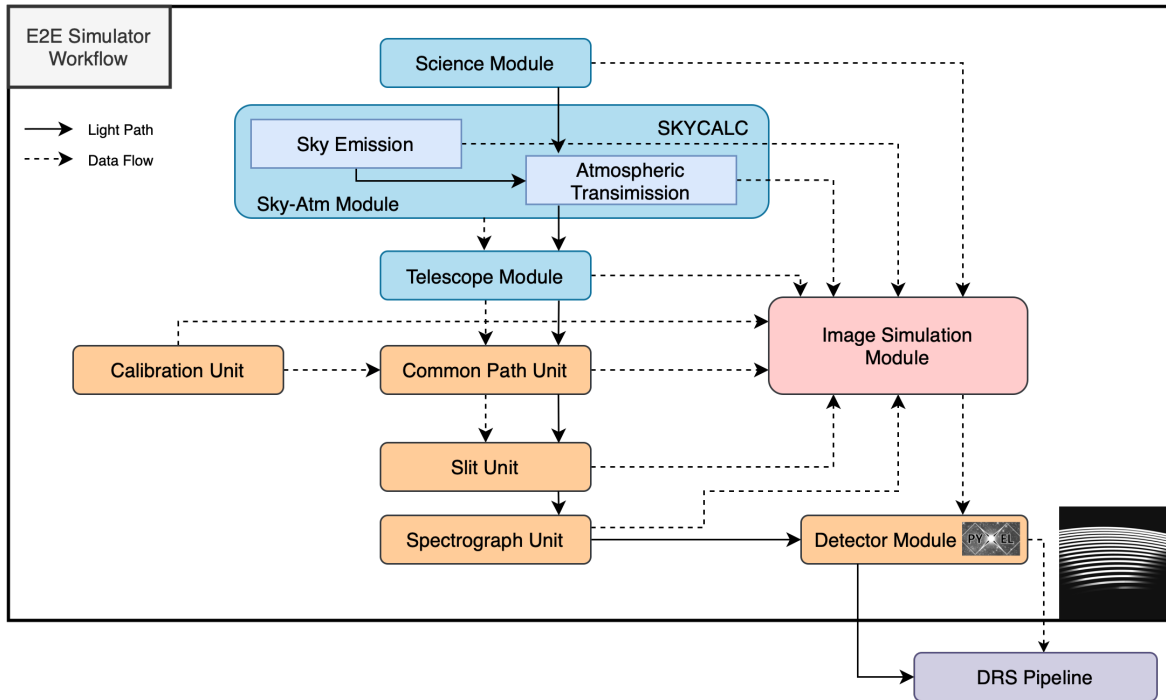


Figure 2: E2E simulator workflow schematic description. The solid arrows represent the real light path, while the dashed arrows show: the simulation data-flow, how the different modules and units are interfaced and their connection to the simulator core, which is the Image Simulation Module. Orange blocks are units of the Instrument Module, while blue blocks are related to simulation modules independent from the specific instrument.

### 3.1 The Simulator Architecture

In the following a brief description of the modules and units showed in the workflow diagram is given; more details can be found here.<sup>5</sup>

#### 3.1.1 Science Module

It generates a synthetic 1D spectrum of an astronomical source for a user-defined set of parameters (e.g. flux distribution, magnitude), at a resolution higher than the selected instrument mode (i.e. HR or LR). A user-defined spectrum (in ASCII format) can also be uploaded as the input spectrum, where the user must ensure that the resolution is again greater than that of the selected HR or LR mode.

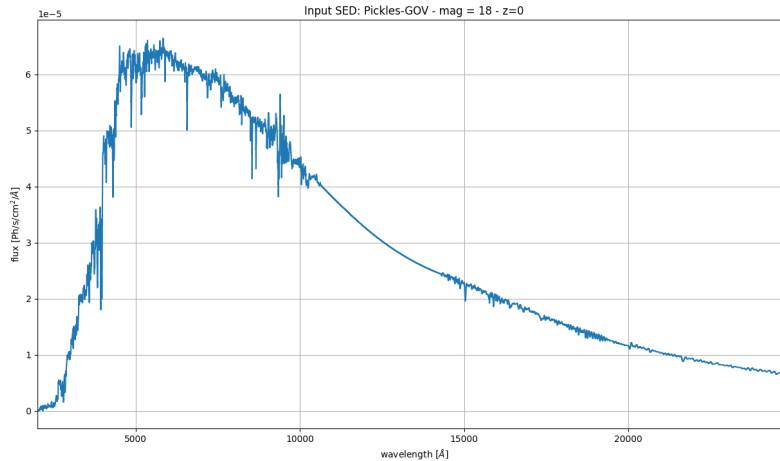


Figure 3: Example of a synthetic 1D spectrum for a G0V star (Pickles model) sampled at resolution of  $0.5 \text{ \AA}$ , mag 18 (V band of Johnson-Cousins filters, in Vega magnitude system) and at  $z = 0$ .

### 3.1.2 Sky-Atmosphere Module

Spectra are modelled by the Sky-Atmosphere module invoking a dedicated library built using the ESO skycalc tool (REFF-SkyCalc). These spectra are loaded from the library according to the adopted observing conditions for the simulation, i.e. moon phase, airmass and precipitable water vapour.

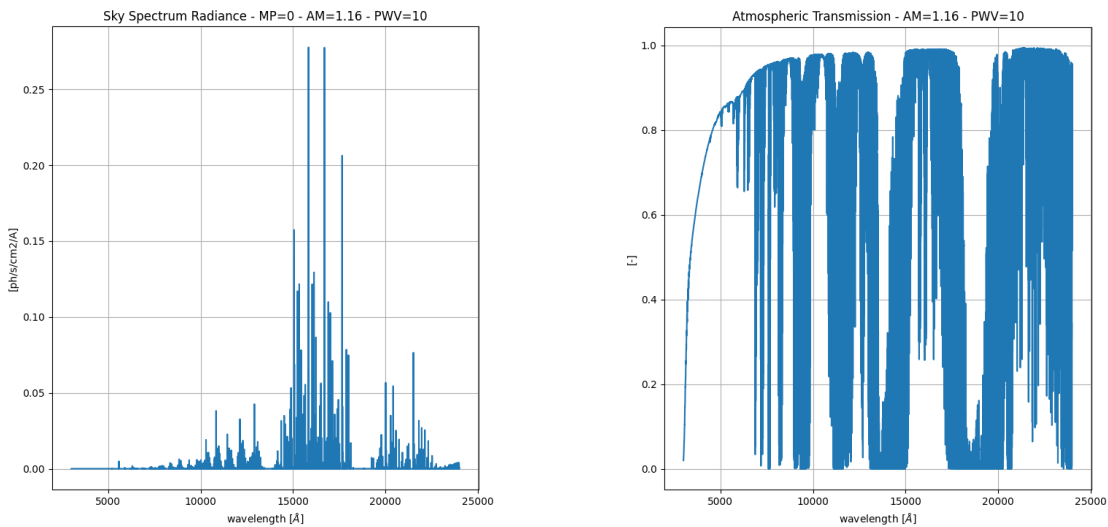


Figure 4: Example of a sky radiance spectrum and atmospheric transmission calculated through the ESO-SkyCalc tool. New moon, air-mass=1.16 and precipitable water vapor (PWV) = 10 mm

### 3.1.3 Instrument Module

The instrument module is composed of the fore-optics, slicer and spectrograph units. The slicer unit computes the slit efficiency, i.e. the fraction of light passing through the pseudo-slit reformatted at the spectrograph entrance slit. This is related to the design configuration and/or resolution mode, where the HR slicer provides an on-sky

field-of-view of  $1.5'' \times 10''$  and the LR slicer has a larger field of  $6'' \times 10''$  (as described by<sup>4,6</sup>). The calculation of the slit efficiency is implemented taking into account the instrument entrance aperture sizes (width and length), the optical quality (PSF FWHM) of the optical path up to the slicer focal plane and the seeing (FWHM at 500 nm). Optionally, the PSF can be convolved with a given spatial profile, which is useful to simulate the appearance of extended targets. The spectrograph unit predicts the spectral format at the focal plane of the two CUBES arms, the instrument throughput, and a database of PSF maps for a set spectral resolution element (which are used by the Image Simulation Module to render the synthetic frames). The spectrograph unit extracts the slice traces (position and orientation along the main dispersion direction) and the slice PSF maps from the Spectrograph Optical File(s) designed in Zemax-OpticStudio®. The accuracy of the aberrations, distortion, and diffraction effects is determined by the parameters used to run the specific optical design files.

### 3.1.4 Image Simulation Module

This module is responsible of rendering the photon distribution for each spectral resolution element for each slice at the level of the focal plane of the spectrograph arms. The photons collected by each slice are mapped into separate spectral traces on the detector, applying the input template for the target and the sky to reconstruct the spectral features. This module first interpolates all of the instrumental data produced by other modules on a sub-pixel scale (of which the oversampling can be set according to the required simulation accuracy). It then produces the photon distribution for each wavelength at a sub-pixel scale by convolving each slice image with the corresponding PSF map. Each spectral PSF map is computed by interpolating a grid of PSF maps extracted by the Instrument Module from optical ray-tracing software. The spectral slice images are properly sized and tilted according to the sampling and tilt variation along the main dispersion direction, and scaled for the integrated spectral flux and efficiency. The code architecture has been developed in order to properly exploit the functionality of numba<sup>7</sup> and to take advantage of the parallel features of the concurrent Python package, such that the different slices (or a fraction of them) can run in parallel. Once all the spectral images have been piled up to sum their photons distribution at sub-pixel scale, the synthetic frame is re-binned to pixel scale. Then, the photon noise and all other specific detector noises are added by the Detector Module. In the current development read-out noise (RON), dark current (DC), bias levels, pixels response non-uniformity (PRNU) and pixel cross-talk (due to charge diffusion) are implemented.

### 3.1.5 Detector Module

The detector module utilizes the Pyxel simulation framework<sup>8</sup> to model various detector effects on rendered data at the pixel level. This tool operates through a series of cascading modules that simulate the entire detection chain. For instance, shot noise can be modeled at the photon collection level, while quantum efficiency (QE), dark current (DC), and cosmic ray effects are incorporated at the charge generation level. Additional effects such as read-out noise (RON), bias levels, fixed pattern noise (caused by pixel non-uniform response, PRNU), and pixel cross-talk (due to charge diffusion) can be added at different stages of the simulation. This framework also enables the generation of bias and dark frames for calibration purposes. For 9K-10  $\mu\text{m}$  detectors, the expected dark current (DC) is 0.5 e-/pixel/hour (at a temperature of 165K), the adopted read-out noise (RON) is 2.5 e-rms (at 50 kHz), and a pixel-response non-uniformity of 3% is assumed based on the manufacturer's data sheet.

## 4. ACTIVE FLEXURE COMPENSATION SYSTEM

### 4.1 Description

The Active Flexure Compensation (AFC) functionality is meant to address the following issues:

- Ensure the daytime calibration is valid to reduce night-time data. The accuracy required is 0.01 pixels along the spectral direction and 0.2 pixels along the spatial direction.
- Avoid spectral resolution and efficiency loss due to mechanical flexures of the instrument during the exposure.

In order to achieve these goals, the procedure takes into account two reference spectra (one for each arm of the spectrograph) of the AFC lamp, taken with the telescope in the parking position, and associated to the latest wavelength calibration files. During observations, the rigid shifts of the AFC spectra in both spatial and spectral directions will be analyzed (Sect. 4.2). When flexures due to telescope attitude are detected, the AFC actuators will be used to compensate their effect.

We expect to acquire AFC spectra images continuously during science observations, i.e. the AFC lamp will always be ON during operations. A first correction will always be applied after the target has been acquired but before the observation template is started. Successive corrections will be applied by performing a trend analysis over 10 AFC acquisitions and over a timespan of at least 10 minutes. If the exposure remaining time is less than 10 minutes, or if the whole exposure time is less than 10 minutes, no AFC correction will be applied.

The image of the AFC spectrum in this initial acquisition, as well as the image of the last AFC acquisition (if present) will be attached as an extension to the science FITS file for further analysis by the DRS (e.g. to correct for second order effects such as spectral “breathing”).

## 4.2 Cross-correlation Algorithm

The CUBES control software shall be able to estimate the shifts (in both spatial and spectral directions) of the AFC lamp spectrum as seen on both science detectors during observations. The algorithm works as follows:

1. A reference spectrum of the AFC lamp is taken during daytime calibrations, with the telescope in the parking position and a high SNR;
2. During night-time observations, a new spectrum of the AFC lamp is taken at regular intervals, with a low SNR;
3. The region of the observation and reference images containing the spectrum, spanning 9200 x 60 pixels, is selected. This region will not change significantly with flexures, since the shifts are expected to amount at most to a few (<5) pixels;
4. The bias is subtracted from the observation and reference images;
5. The image regions with the observation and reference spectra are cross-correlated, with a lag spanning 50 pixels in both spectral and spatial directions: this results in a 2D array (50 × 50) of the cross-correlation (Figure 6, upper left panel);
6. The 2D cross-correlation array has a peak whose position depends on the shift between the observation and reference spectra: to find the position with sub-pixel accuracy, a 2D gaussian fit is performed (Figure 6), thus finding the center parameter providing the best fit value for the shift in the spectral and spatial direction.

## 4.3 Results

In order to test the accuracy of the algorithm in estimating the shifts, a set of simulations obtained with the CUBES End-to-end (E2E) simulator was used. Specifically, reference and observation frames of the Active Flexure Compensation (AFC) were generated, considering the spectrum of a ThAr lamp using Photron lines as reference. Observation frames were generated with multiple rigid shifts in the spectral and spatial direction and an exposure time equal to one-tenth of that of the reference frame. As a first simulation step and to aid the development of the cross-correlation algorithm, the frames were provided without overscan regions.

As shown in Figure 7, the distribution of the best fit values for the center of the 2D model curve shows that the algorithm is able to estimate the shift with the required accuracy of 0.01 pixels along the spectral direction and 0.2 pixels along the spatial direction.

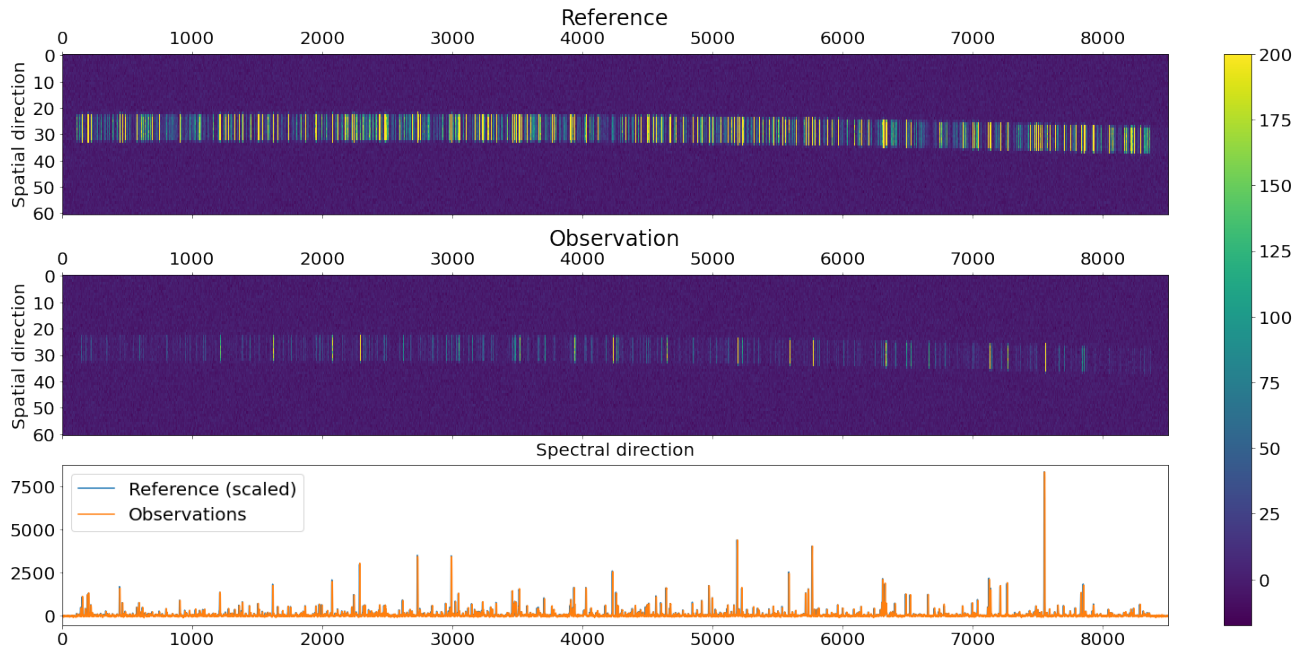


Figure 5: The daytime reference image (upper panel) and the night-time observation image (middle panel). In the lower panel, the reference and observation spectra are shown, obtained by summing each image along the spatial direction.

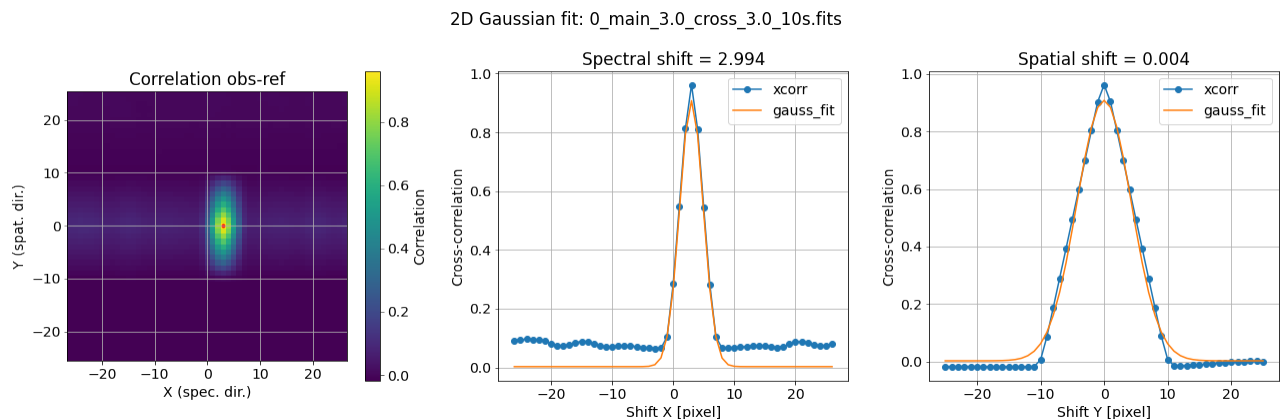


Figure 6: **Left panel:** the 2D cross-correlation between the observation and reference frames. **Middle panel:** a horizontal slice of the 2D cross-correlation (in blue) and of the best-fit model (in orange), at the position of the center. **Right panel:** a vertical slice of the 2D cross-correlation (in blue) and of the best-fit model (in orange), at the position of the center.

## 5. DATA REDUCTION SOFTWARE

The CUBES Data Reduction Software (DRS) is now in the final design phase. It includes three distinct pipelines:

- a pipeline to reduce and extract spectroscopic data, correcting from the detector signature, and performing wavelength calibration, sky subtraction, and standard-star-based flux calibration;
- a pipeline to perform photometry on the A&G images, in order to improve the absolute flux calibration of the spectroscopic data;
- a pipeline to monitor the instrument health status, performing wavelength calibration and checks on the detector linearity.



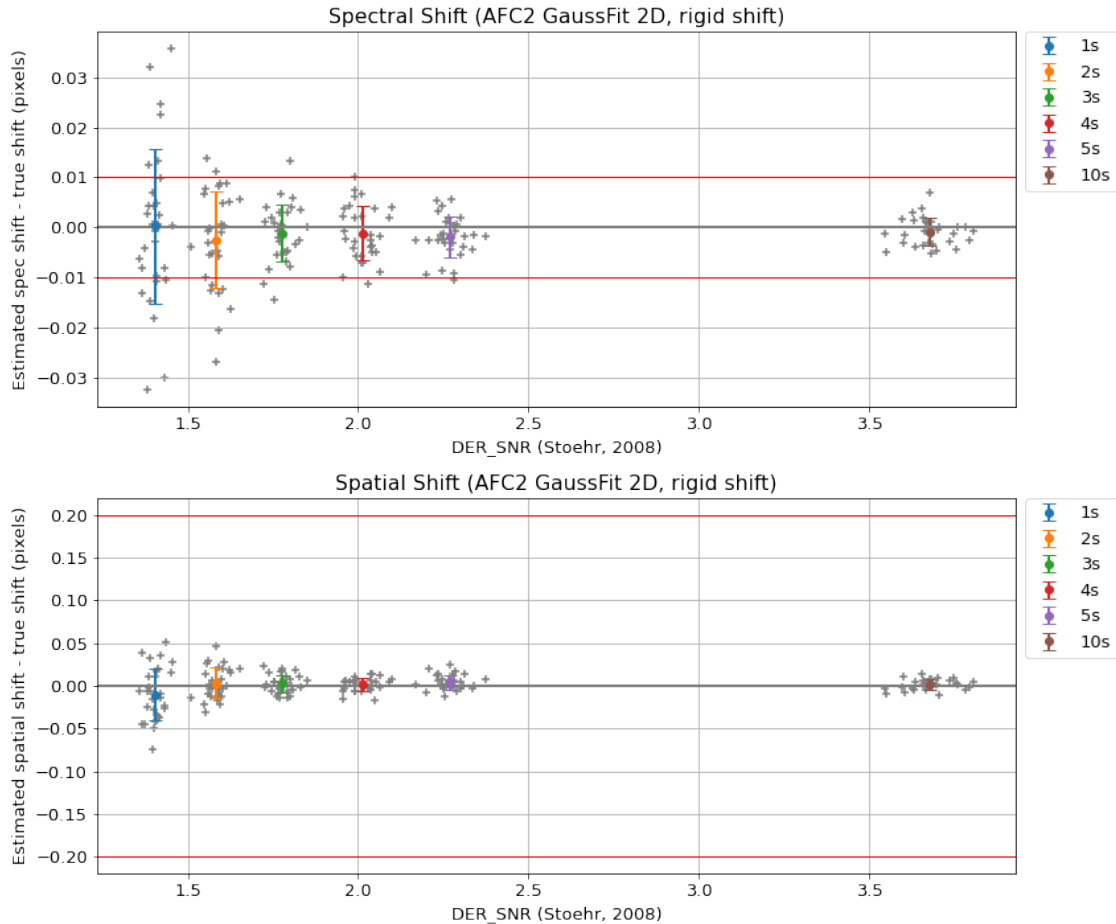


Figure 7: The result of the test of the AFC algorithm with simulated images. In the upper panel, the difference between the estimated spectral shift and the real value is shown, with each gray cross corresponding to a single image and the dots with error bars corresponding to the mean  $\pm\sigma$ . In the lower panel, the same plot for the spatial direction. Red lines show the required accuracy.

A schematic representation of the joint spectroscopy+photometry workflow is given in Figure 8.

The core of the DRS is the set of “recipes” highlighted by a bold contour in Figure 8, which implement the following critical algorithms:

- **Wavelength calibration:** a set of isolated, high-SNR ThAr lines are detected in a calibration spectrum and fitted in with a bivariate spline, to obtain the 2-d map between positions in the detector space and wavelengths. All pixels in the 6 slices are thus assigned a calibrated wavelength.
- **Sky modeling:** the emission spectrum of the sky (continuum and lines) is sampled using the spatial extension of the slices,<sup>9</sup> either directly on the science target observation or on a dedicated sky observation, and smoothed with a B-spline.
- **Flux calibration:** the response curve of the instrument is interpolated at the wavelength of all pixels in the slices, to convert electron counts in flux units. After extraction, flux calibration is further improved by using the photometry from the A&G camera.
- **Extraction and co-addition:** an optimal-extraction algorithm<sup>10</sup> is combined with a “drizzling-like” technique to weight the contributions to each wavelength bin in the final spectrum,<sup>11</sup> maximizing the SNR per resolution element while preserving flux calibration.

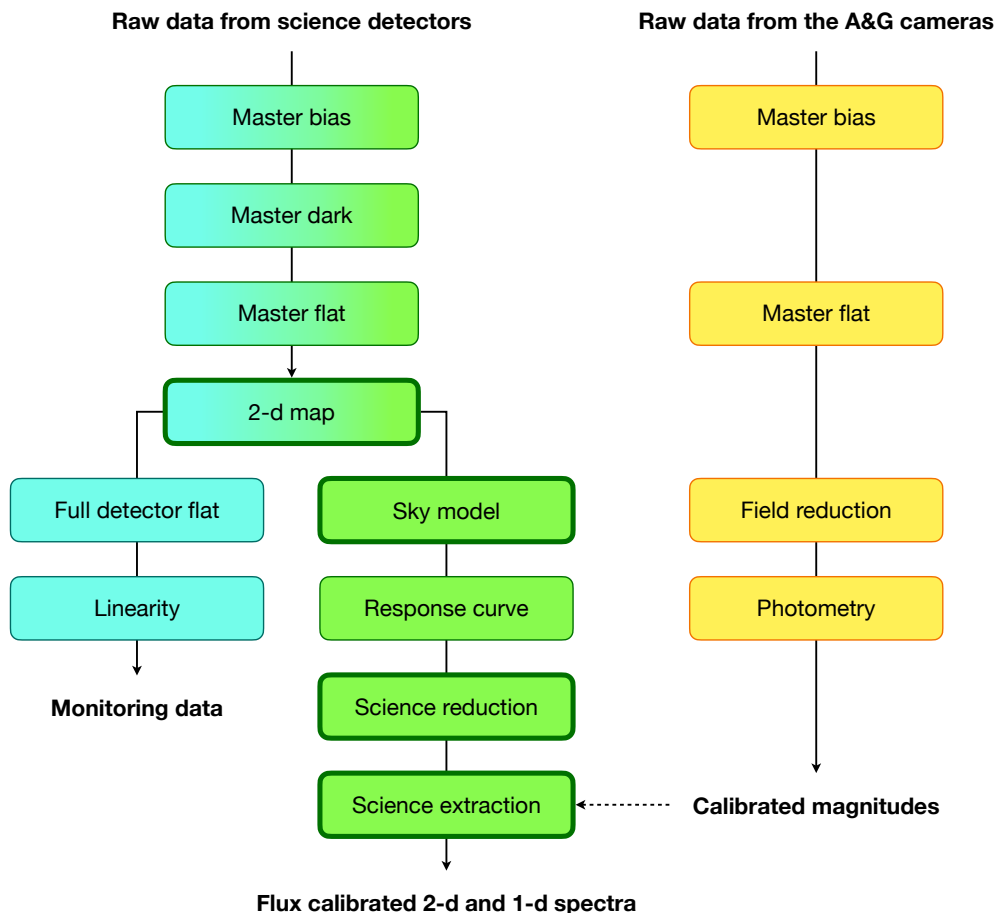


Figure 8: Scheme of the DRS workflow. Each box represents a unitary operation on instrument data (“recipe”). The spectroscopy and monitoring pipelines are shown in green and turquoise, respectively (part of the cascade is shared between the two pipeline, as denoted by shading), while the photometry pipeline is shown in yellow. The connection between spectroscopy and photometry takes place within the extraction recipe, which accepts magnitudes measured on the A&G images as a way to improve flux calibration of science spectra.

Already during Phase C, a complete prototype of the critical algorithms has been implemented (as a suite of Python scripts and Jupyter notebooks<sup>12</sup>). Some products of the prototype pipeline are given in Figures 9, 10, and 11, showing respectively the result of extraction and co-addition of spectra, the SNR achieved by different extraction techniques, and the accuracy of wavelength calibration. These products are obtained from the simulated frames shown in Figure 12, and the results demonstrate how the prototype pipeline (and the full DRS when it is implemented) is an essential complement to the E2E simulator, effectively closing the loop from the input template spectra to the final extracted products. Throughout the integration phase, the joint E2E+DRS infrastructure will be pivotal in checking the performances of both the simulator and the reduction algorithms.

The final version of the DRS, to be released by ESO after the instrument commissioning, will be implemented using the ESO Common Pipeline Library (CPL)\* and will be accessed through the new Python-based ESO Data Processing System (EDPS).<sup>13</sup>

\*<https://www.eso.org/sci/software/cpl/>.

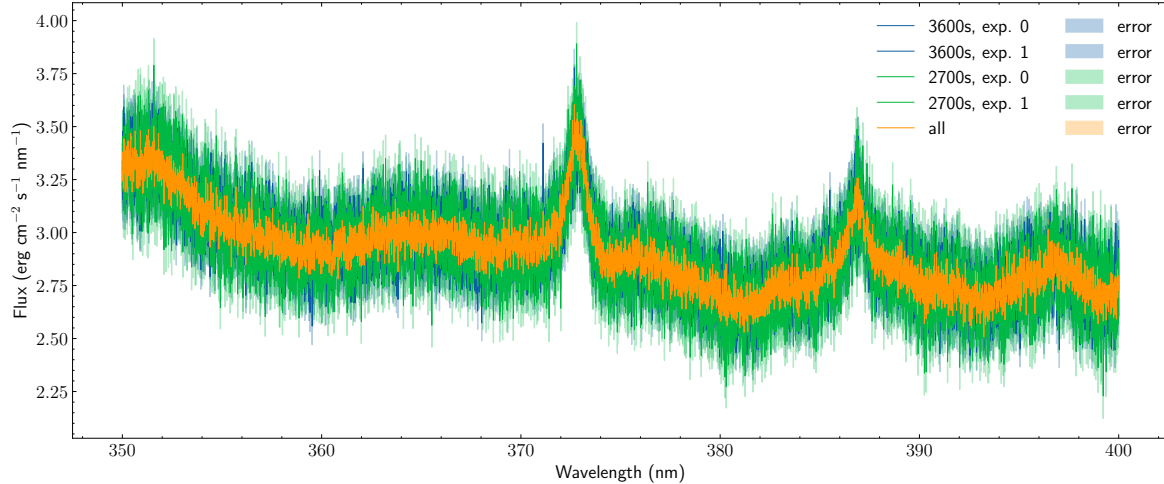


Figure 9: Extracted quasar spectra, produced by the prototype pipeline from E2E simulated data. The purpose is to compare the result of the extraction for individual exposures of the same target (blue and green; integration time of 3600 s and 2700 s respectively) with the co-added spectrum obtained by extracting all exposures at once (orange). The increase in SNR is apparent, as well as the preservation of the correct flux levels.

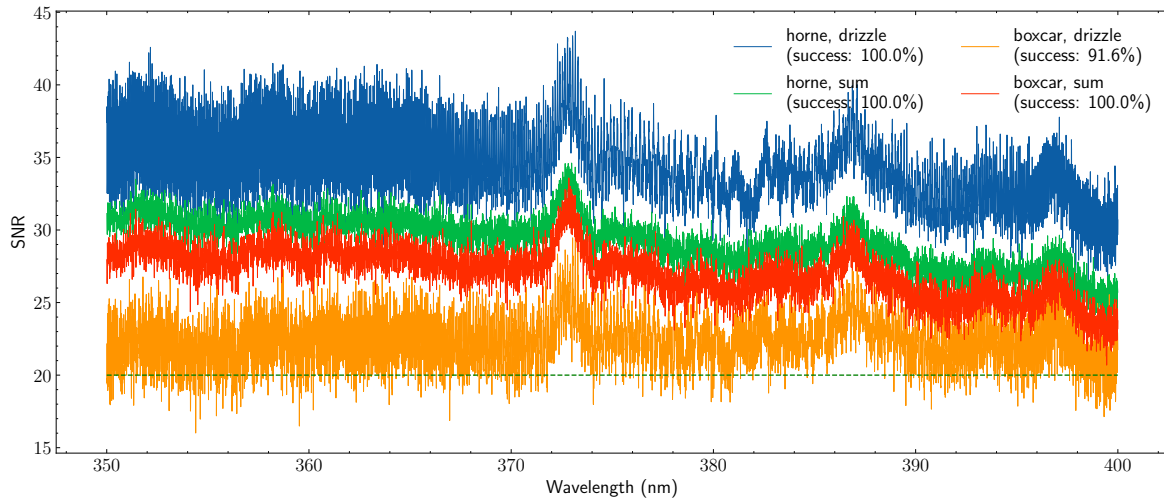


Figure 10: SNR obtained with different extraction techniques, namely (cf. text): (i) drizzling with Horne-like weighting (blue), (ii) sum with Horne-like weighting (green), (iii) drizzling with boxcar weighting (orange), and (iv) sum with boxcar weighting (red). The advantage of the first approach is apparent. The dashed line shows the threshold SNR to be achieved on a 18 magnitude target in 3600 s, according to the top-level requirements for the instrument.

## 6. CONCLUSION

CUBES will provide unprecedented spectroscopic sensitivity in the bluest part of the spectrum that can be observed from the ground. In this paper, we detailed the architecture and capabilities of the CUBES E2E instrument simulator, illustrating the specific tasks and functionalities of its various modules. We emphasized the collaborative efforts between the E2E and DRS teams in evaluating the performance of both the simulator and the reduction algorithms. Furthermore, we demonstrated that the cross-correlation algorithm for the AFC system accurately retrieves shifts in both spatial and spectral directions in the simulated frames. Moving forward, we will continue our collaboration with the DRS team to test upcoming recipes, such as the flux calibration, and plan to evaluate the AFC cross-correlation algorithm under more challenging conditions, including spectral breathing.

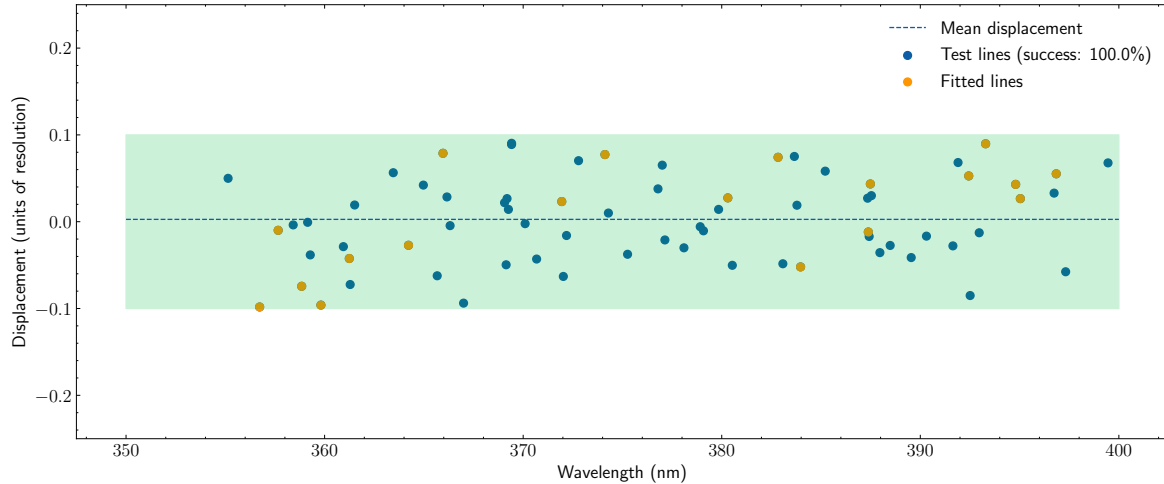
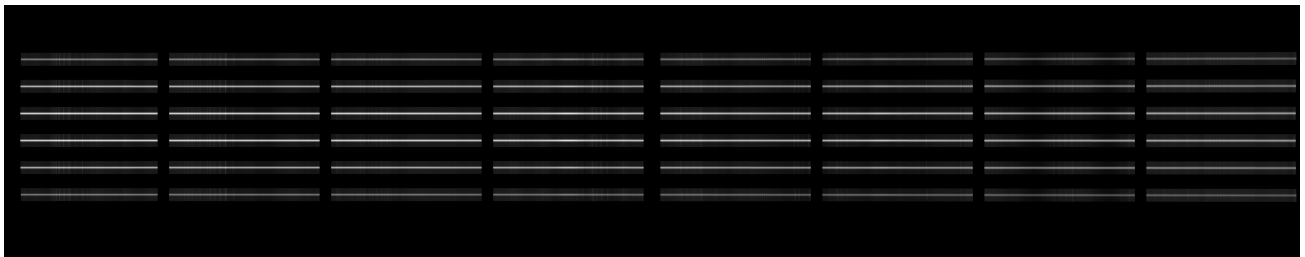
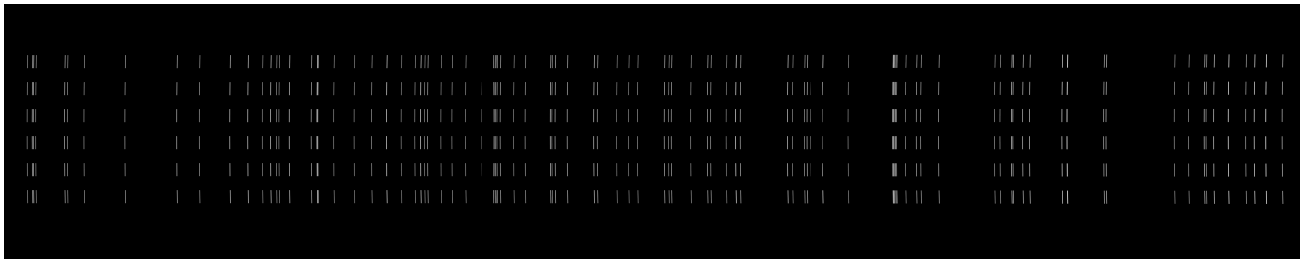


Figure 11: Displacements between laboratory wavelengths of selected ThAr lines and calibrated wavelengths measured on the extracted ThAr spectrum. Orange dots are the lines used to produce the 2-d wavelength map, while blue dots are other test lines used to assess the accuracy of the wavelength calibration. The top-level requirements for the instrument set an accuracy limit of 0.1 resolution elements, corresponding to the green shaded region.



(a) Science frame: QSO object



(b) Calibration frame: Thorium-Argon (ThAr) lamp

Figure 12: Portions of raw simulated frames used in the development of optimal extraction and wavelength calibration recipes. The above image (12a) shows a raw science frame of a QSO object (which also includes sky contribution), while the bottom (12b) shows a raw calibration frame with a Thorium-Argon (ThAr) lamp. The detector noise in the original frames has been removed for better visualization.

## REFERENCES

- [1] Evans, C. J., Barbuy, B., Castilho, B., Smiljanic, R., Melendez, J., Japelj, J., Cristiani, S., Snodgrass, C., Bonifacio, P., Puech, M., and Quirrenbach, A., “Revisiting the science case for near-UV spectroscopy with the VLT,” in [*Ground-based and Airborne Instrumentation for Astronomy VII*], Evans, C. J., Simard, L., and Takami, H., eds., **10702**, 107022E, International Society for Optics and Photonics, SPIE (2018).
- [2] Opitom, C., Snodgrass, C., Forgia, F. L., Evans, C., Cambianica, P., Cremonese, G., Fitzsimmons, A.,

- Lazzarin, M., and Migliorini, A., “Cometary science with CUBES,” **55**, 59–73, *Experimental Astronomy* (2023).
- [3] Genoni, M., Landoni, M., Cupani, G., Franchini, M., Cirami, R., Zanutta, A., Evans, C., Marcantonio, P. D., Cristiani, S., Trost, A., and Zorba, S., “The cubes instrument model and simulation tools. their role in the project phase a study,” (2022).
- [4] Genoni, M. et al., “Cubes, the cassegrain u-band efficient spectrograph: Towards final design review.,” *Proc. SPIE* **13096-296** (2024).
- [5] Genoni, M., Scaudo, A., et al., “Progress on the simulation tools for the soxs spectrograph: Exposure time calculator and end-to-end simulator,” (2022).
- [6] Calcines, A., Wells, M., O’Brien, K., Morris, S., Seifert, W., Zanutta, A., Evans, C., and Marcantonio, P., “Design of the vlt-cubes image slicers;,” *Experimental Astronomy* **55**, 1–14 (09 2022).
- [7] Lam, S. K., Pitrou, A., and Seibert, S., “Numba: A llvm-based python jit compiler,” in [*Proceedings of the Second Workshop on the LLVM Compiler Infrastructure in HPC*], *LLVM '15*, Association for Computing Machinery, New York, NY, USA (2015).
- [8] Arko, M., Prod’homme, T., Lemmel, F., Serra, B., George, E. M., Kelman, B., Pichon, T., Biancalani, E., and Gilbert, J., “Pyxel 1.0: an open source Python framework for detector and end-to-end instrument simulation,” *Journal of Astronomical Telescopes, Instruments, and Systems* **8**(4), 048002 (2022).
- [9] Kelson, D. D., “Optimal Techniques in Two-dimensional Spectroscopy: Background Subtraction for the 21st Century,” *PASP* **115**(808), 688–699 (2003).
- [10] Horne, K., “An optimal extraction algorithm for CCD spectroscopy.,” *PASP* **98**, 609–617 (1986).
- [11] Cupani, G., D’Odorico, V., Cristiani, S., et al., “Integrated data analysis in the age of precision spectroscopy: the ESPRESSO case,” *Society of Photo-Optical Instrumentation Engineers (SPIE) Conference Series* **9913**, 99131T (2016).
- [12] Kluyver, T., Ragan-Kelley, B., Pérez, F., et al., “Jupyter notebooks – a publishing format for reproducible computational workflows,” 87 – 90, IOS Press (2016).
- [13] Freudling, W., Zampieri, S., Coccatto, L., et al., “Adaptive data reduction workflows for astronomy: The ESO Data Processing System (EDPS),” *AAP* **681**, A93 (2024).